



UNIVERSITÀ  
DEGLI STUDI  
DI PADOVA

*Università degli Studi di Padova*

*Padua Research Archive - Institutional Repository*

Enhancement of corrosion resistance to sterilization stages of a  
biomedical grade AISI 316L stainless steel by means of lowtemperature

*Original Citation:*

*Availability:*

This version is available at: 11577/3296370 since: 2019-04-09T13:50:51Z

*Publisher:*

*Published version:*

DOI:

*Terms of use:*

Open Access

This article is made available under terms and conditions applicable to Open Access Guidelines, as described at <http://www.unipd.it/download/file/fid/55401> (Italian only)

(Article begins on next page)



BioM&M\_2018

# Enhancement of corrosion resistance to sterilization stages of a biomedical grade AISI 316L stainless steel by means of low-temperature machining

R. Bertolini\*<sup>a</sup>, S. Bruschi<sup>a</sup>, A. Ghiotti<sup>a</sup>

<sup>a</sup>*Dept. of Industrial Engineering, University of Padova, Via Venezia 1, 35131, Padova, Italy*

---

## Abstract

Austenitic stainless steels are currently used for the manufacture of reusable medical instruments, thanks to their combination of elevated strength, corrosion resistance, biocompatibility and low cost. However, during their service life, they are subjected to repeated sterilization cycles, which lead to the loosening of the surface oxide stability and, as a consequence, the decrease of their durability.

In the present study, the in-service corrosion behaviour of the AISI 316L stainless steel was investigated after being machined using two low-temperature coolants, namely Liquid Nitrogen (LN<sub>2</sub>) and gaseous Nitrogen (N<sub>2</sub>) cooled by LN<sub>2</sub> to -100°C, as well as using a conventional cutting fluid.

Results showed that the AISI 316L microstructure near the machined surface was significantly affected by the machining cooling strategies with the generation of a hardened and more compressed layer when low-temperature coolants were used. Such surface integrity enhancements contributed to improve both the general and localized corrosion resistance to sterilization stages. From this basis, machining using low temperature coolants can be considered a suitable technique to manufacture medical devices of increased durability.

© 2018 Elsevier Ltd. All rights reserved.

Selection and Peer-review under responsibility of 1st International Conference on Materials, Mimicking, Manufacturing from and for Bio Application (BioM&M).

*Keywords:* Stainless steel; cryogenic machining; corrosion; pitting

---

## 1. Introduction

Austenitic stainless steels have been widely used in the biomedical field thanks to their mechanical properties, resistance to wear, low reactivity, and modest cost [1]. Austenitic 304 and 316 steels (SS304 and SS316) have

been used to make a wide range of medical devices, including coronary stents, hip implant stems, spinal disc replacements, and fracture fixations, as well as surgical tools, such as needles, scalpels, blades, curettes, forceps, and retractors [2]. Nevertheless, during their service life, they are subjected to both mechanical stress and cyclic sterilization stages, which drastically contribute to reduce their durability.

Various techniques have been exploited with the objective of improving surface properties: coating [3], nitriding [4] and carburization [5] processes were used to increase the corrosion performance of austenitic stainless steels, even if these methods are complex to be carried out and expensive. The surface characteristics of biomedical devices play a fundamental role in governing the corrosion resistance and recent works have demonstrated that they can be suitably modified through finishing machining processes [6]. In particular, Liquid Nitrogen (LN2) has emerged as a machining cooling strategy capable to improve the functional characteristics of those metallic materials mostly used in biomedical applications (e.g. magnesium, cobalt and titanium alloys) [7][8][9]. In [7], cryogenic burnishing process was used to improve the surface integrity of a Co-Cr-Mo biomedical alloy: results showed a region characterized by grain refinement as a consequence of machining that was 170% thicker when LN2 was applied than in case of dry burnishing. Moreover, micro-hardness measurements indicated that the hardness was increased by 87% in cryogenic burnishing conditions compared to the bulk value. In [10] the corrosion resistance of a magnesium alloy was increased by optimizing specific turning process parameters: cryogenic turning was exploited to obtain a featureless layer in the machined sub-surface, while the feed rate was modified to reduce the aspect ratio of the feed marks characteristic of the turning operation, achieving a decrease of the alloy wettability.

However, in the case of stainless steels, the feasibility of using cryogenic cooling to improve corrosion resistance has not been investigated, yet. To this aim, the present study evaluates the effect of different cooling strategies, namely cryogenic cooling and a newly developed cooling approach based on the use of gaseous Nitrogen (N2) mixed with LN2 in order to reach a temperature of  $-100^{\circ}\text{C}$ , on the corrosion resistance of an austenitic stainless steel to the sterilization stages typical of reusable surgical instruments. Dry and wet cutting were also used as baseline. Results show that the reduction of an order of magnitude in the corrosion current and an increase in the pitting potential was achieved by using liquid nitrogen-based coolants; in this way the durability of reusable devices can be successfully increased.

## 2. Experimental

### 2.1. Material under investigation

The material under investigation was the biomedical grade AISI 316L stainless steel, supplied in form of bars of 50 mm of diameter and 600 mm of length.

Table 1 reports the main mechanical characteristics of the AISI 316L in the as-delivered conditions.

Table 1. Mechanical properties of the as-delivered AISI 316L.

Material	E (GPa)	Y(MPa)	Elongation (%)	Poisson's ratio	HV <sub>0.01</sub>
AISI 316L	195	262	40	0.31	127

### 2.2. Machining tests

The machining experimental campaign was conducted on a Mori Seiki<sup>TM</sup> CNC lathe. The utilized cutting tool insert was a CNMG 120404-MF 1125 semi-finishing insert with a radius of 0.4 mm, mounted on a PCLNR 2020 K12 tool holder with an approach angle of  $95^{\circ}$ , both supplied by Sandvik Coromant<sup>TM</sup>. Both the insert grade and micro-geometry were chosen on the basis of the tool manufacturer's guidelines for machining stainless steels. The values of the cutting speed ( $V_c$ ), feed ( $f$ ) and depth of cut ( $d$ ) were equal to 200 m/min, 0.2 mm/rev and 0.3 mm, respectively. A fresh cutting edge was used for each trial, with a machining time slightly higher than 1 minute, but anyway not sufficient to determine a significant tool wear. The turning tests were carried out using two different low-temperature cooling strategies, based on the use of LN2 and cooled N2, besides of the standard

dry and wet conditions. Two separated self-designed lines were developed and implemented on the CNC lathe for the abduction of the low-temperature coolants. The first experimental apparatus, patented by Air Liquide Service Italy and called Cryofluid™, allows cooling the gaseous N<sub>2</sub> in the range between 0°C and -150°C in an insulated chamber where the N<sub>2</sub> is mixed with the LN<sub>2</sub> until reaching the desired temperature. The maintenance of the gaseous N<sub>2</sub> at the desired temperature during the whole test is guaranteed by a retroactive temperature control making use of an internal PLC controller. In this work a testing temperature of -100°C was considered, the output coolant pressure was fixed constant at 2.5 bars, and the cutting zone was cooled with one nozzle with an internal diameter of 6 mm directed onto the tool rake face [11].

The second experimental apparatus instead, is a liquid nitrogen cooling system, which includes a Dewar, a control unit, and a distribution system made of plates mounted on the lathe turret designed to deliver the coolant at 4 l/min and 15 bars to the tool rake and flank faces using two external copper nozzles with an internal diameter of 0.9 mm [12].

Table 2 summarizes the parameters adopted during the experimental campaign.

Table 2. Summary of the parameters adopted during the experimental campaign.

Machining parameters (fixed)		Machining tests	
Cutting insert	CNMG 120404-MF 1125		Dry
Cutting speed (m/min)	200		Wet
Feed (mm/rev)	0.2	Cooling conditions	LN <sub>2</sub> (-100°C)
Depth of cut (mm)	0.3		N <sub>2</sub>

### 2.3. Characterization after machining

#### 2.3.1 Mechanical characterization

The residual stresses on the cylindrical machined surfaces were determined by means of the X-Ray Diffraction (XRD) technique with CuK $\alpha$ -radiation using the (2,2,0) interference lines. The analysis was based on the  $\sin 2\psi$ -method [13] for which the lattice spacing was measured at five  $\psi$ -angles between  $-35^\circ$  and  $+35^\circ$ . The residual stresses from the observed lattice strains were calculated on the basis of the mechanical properties in the as-delivered conditions reported in Table 1. The samples for the X-ray analysis were degreased in ultrasounds and fixed on a sample holder. The measurements were performed using a Spider™ X GNR portable diffractometer working at 30 KV and 90  $\mu$ A. The counting time for each of the five measures at the different  $\psi$ -angles was 500 s. The depth distribution of the residual stresses was determined by electrolytic removal of thin surface layers and subsequent X-ray measurements. The electrolytic polishing was performed using as electrolyte a solution containing 90 ml of water, 730 ml of ethanol, 100 ml of butoxyethanol and 78 ml of perchloric acid working at 50 V for one minute and maintaining the temperature of the electrolyte at 20°C. Tests were repeated three times in order to assure repeatability.

Vickers micro-hardness measurements were carried out using a Leitz Durimet™ micro-hardness tester with a load of 98 mN for 30 s; three values were recorded and then the average value calculated. In order to investigate the effect of the cooling strategy, the measurements were carried out at a distance of 20  $\mu$ m from the machined surface.

#### 2.3.2 Surface defects examination

The mapping of the machined surface defects was performed using the FEI QUANTA 450™ Scanning Electron Microscope (SEM) with the Back-Scattered Electron Detector (BSED) probe in order to detect the possible presence of adhered material. At least ten images, taken in different zones and acquired at different magnifications, namely 500X and 1000X, were used to characterize the sample surface.

### 2.3.3 Corrosion tests

The electrochemical behaviour was studied using a standard three electrodes cell, where the machined samples were the working electrode, a Saturated Calomel Electrode (SCE) the reference electrode, and a platinum electrode the counter electrode. An Amel<sup>TM</sup> 2549 potentiostat was used for the electrochemical tests. The potentiodynamic polarization curves were obtained from a starting potential of 0.3 V below the Open Circuit Potential (OCP) to a potential of 1 V, at a scan rate of 0.5 mVs<sup>-1</sup>.

The potentiodynamic polarization curves were obtained through testing in a commercial sterilizing solution applied for the disinfection of medical instruments (IGENAL-N), whose main constituents included dodecyl-dimethyl ammonium chloride, quaternary ammonium propionate and polyanethylen biguanide hydrochloride.

The corrosion potential ( $E_{corr}$ ) and the corrosion current density ( $I_{corr}$ ) were determined from the polarization measurements using the Tafel extrapolation method, according to the ASTM G5-14 standard [14]. The potentiodynamic polarization curves were repeated three times in order to assure the results reproducibility.

The susceptibility to localized corrosion was evaluated through cyclic polarization tests, following the ASTM G-61 [15] and ASTM F746 [16] standards. The corrosion cell and electrolyte were the same used for the potentiodynamic polarization tests. First, the samples were stabilized for one hour at OCP condition, and then the potential scan was performed at 10 mV\*s<sup>-1</sup> in the anodic direction, from a potential from -0.5 V to 1.5 V.

## 3. Results and discussion

### 3.1. Mechanical characteristics

Fig. 1 a) shows the depth profiles of the residual stresses. It is worth to underline that, even if residual stresses were measured in both radial and axial directions, here results are reported in the radial direction since they are characterized by greater differences. The curves reported in Fig. 1 present the same general trend for all the conditions, with an initial sharp decrease and subsequent increase until reaching values close to zero approximately at 200  $\mu\text{m}$  from the machined surface. The presence of compressive residual stresses in the radial direction is highlighted regardless of the cutting condition; anyway, a strong effect of the thermal field arising during cutting can be observed. In fact, as reported in Fig. 1 b), the maximum residual stress ( $\sigma_{max}$ ) is 486 MPa (compressive) in dry condition, decreases to 576 MPa (compressive) in wet condition, and is further reduced to 808 MPa (compressive) and 882 (compressive) in the N<sub>2</sub> and LN<sub>2</sub> cases, respectively.

The residual stresses area ( $A_{rs}$ ), which refers to the area under the residual stresses curve, is significantly higher at the lowest temperature compared to the dry and wet conditions. Similarly, the thickness of the layer affected by residual stresses is higher if liquid nitrogen is applied during machining.

Residual stresses are one of the most significant surface parameters regarded in order to improve performances and service life of the components, especially to enhance fatigue strength. It was demonstrated that liquid nitrogen can be used as a mean to obtain large compressive residual stresses at a deep level below the surface [17]. In particular, in the case of stainless steels, which are often regarded as difficult-to-machine materials because of their low thermal conductivity, the residual stresses are greatly affected by the heat generated during the finishing machining process [18][19]. Since the rise of temperature due to cutting is limited when using low-temperature coolants, a more compressive residual stress state is induced compared to dry and wet cutting.

Fig. 1 c) reports micro-hardness values as a function of the cooling strategy. In general, a drastic increase in hardness was found, regardless of the cooling condition, compared to the base alloy (see Table 1 for comparison). This can be attributed to the strain hardening induced by cutting. Furthermore, the cryogenic machined sample presents the highest hardness with an increase of 17% compared to the dry condition while the other conditions settle to comparable values. Similar evidences are confirmed by previous research studies. In [20], cryogenic machined samples showed higher hardness as a consequence of the combination of reduced thermal softening effect and greater grain refinement. These enhancements have important implications on durability of medical devices since high surface and sub-surface hardness reduces the wear rate, while large compressive residual stresses improve the fatigue resistance. Generally, pre-machining and post-machining techniques (shot peening, laser peening, roller burnishing, etc.) are used to improve both hardness and compressive residual stresses.

However, these techniques represent an additional step to be carried out in the product process chain. On the contrary, the same outcomes can be achieved by using low-temperature coolants during finishing machining operations without additional processes.

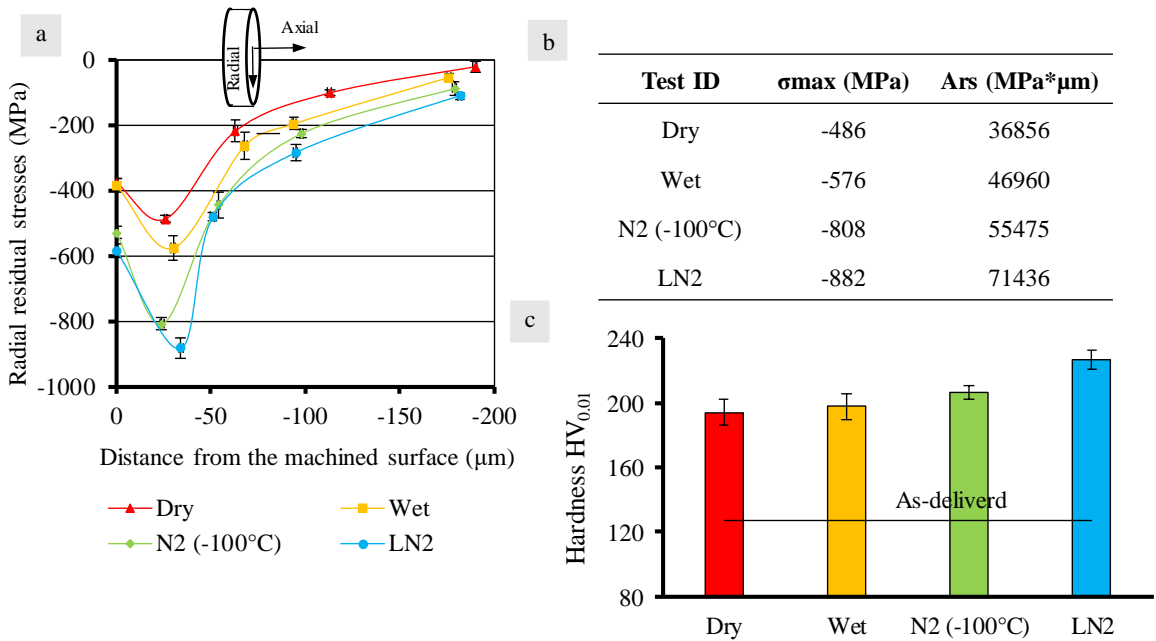


Fig. 1. a) Depth profiles of the radial residual stresses; b) residual stresses parameters as a function of the cooling strategy; c) micro-hardness on the surface as a function of the cooling strategy.

### 3.2. Surface defects

Fig. 2 reports the main defects found on the machined surfaces. Defects such tearings, adhered material, and feed marks irregularities were found on each surface regardless of the cooling strategy, but with different densities. Dry cutting gives the worst surface quality among all the investigated conditions, since it produces the highest amount of all the aforementioned defects. On the contrary, wet, LN2 and N2 machined samples all show a significant increase of the surface quality compared. A slightly lower difference can be highlighted between the use of conventional cutting fluid and the low-temperature coolants, since wet machining promotes the increase of material adhesion and provokes tearing with high dimension. This can be explained by the negative influence of temperature that facilitates the formation of thermally-induced surface defects [21]. On the contrary, the use of low-temperature coolants promotes systematic feed marks irregularities, since low cutting temperatures induce a differential thermal expansion in the cutting area, leading to the material embrittlement.

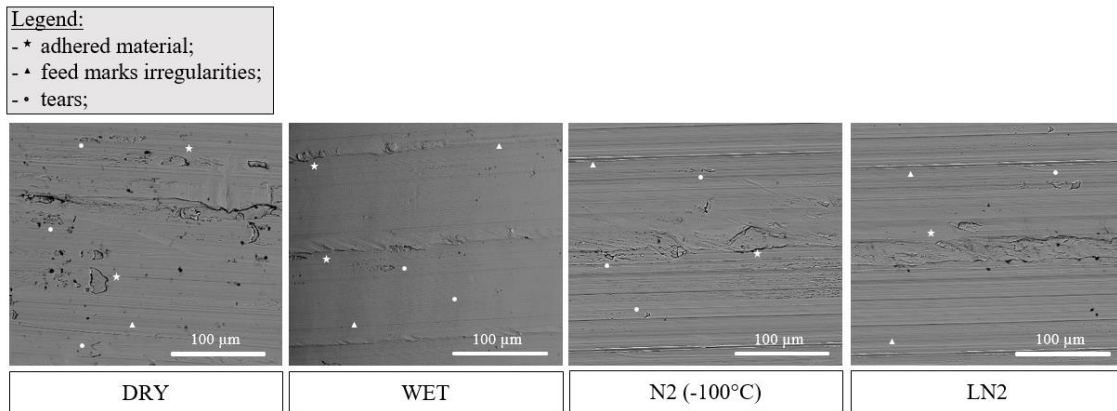


Fig. 2. Examples of surface defects found as a function of the cooling strategy.

### 3.3. Corrosion data

Fig. 3 a) shows that the corrosion behaviour is strictly related to the cooling strategy adopted during machining. In fact, the curves relevant to cryogenic machined samples are shifted towards lower corrosion current values, as can be seen on the magnification reported in Fig. 3a). The corrosion current is a direct indicator of the corrosion rate in aggressive media, being correlated through the Faraday's law. A reduction of an order of magnitude in the corrosion current is achieved when N2 and LN2 are used. Furthermore, a shift to lower currents of the anodic branch can be observed for the samples machined under wet, N2 at -100°C and LN2 conditions if compared with the dry machined one. On the other hand, no significant differences in the corrosion potentials can be observed.

Also the pitting potential ( $E_{pit}$ ) was graphically evaluated from the curves and the results show that the samples with the highest  $E_{pit}$  are the ones cooled through N2 at -100°C and LN2. Since when the critical pitting potential and protection potential decrease, the localized corrosion resistance also decreases, it can be concluded that machining using low-temperature coolants improves the localized corrosion resistance of the machined surfaces.

In order to better analyze the AISI 316L susceptibility to localized corrosion attacks, cyclic polarization tests were performed and the related results reported in Fig. 3c). The area enclosed in the hysteresis cyclic scan can be used as a measure of localized corrosion susceptibility; the larger the hysteresis area the more likely the development of localized corrosion sites [22]. Again, results report that while dry and wet machined samples are characterized by very similar curves, samples machined using N2 at -100°C and LN2 show a nobler behavior since the loop area is drastically reduced, indicating a higher tendency to face localized corrosion phenomena.

Corrosion behaviour is strictly related to the surface generated by the finishing process, since compressive stress has been found to help inhibiting the corrosion phenomena [23]. In [24] different residual stresses states were induced in stainless steels, finding a reduction of the current density thanks to the introduction of a compressive stress state. Compressive residual stresses favor indeed the formation of a strengthened passive film since the compression narrows the interatomic distance.

Also the state of the surface, in terms of amount of surface defects, plays a fundamental role in governing the corrosion resistance. In [25], the correlation between stress corrosion cracking and surface defects was investigated, finding that corrosion was more likely to initiate at pre-existing defects. Substantially, surface defects act as sites for local chemistry changes and stress concentrations that can be precursor of corrosion tearing.

From this basis, it can be concluded that low-temperature coolants applied in machining have two major effects, namely to induce high compressive residual stresses and to minimize the formation of defects, which both contribute, in a synergistic way, to improve their corrosion resistance.

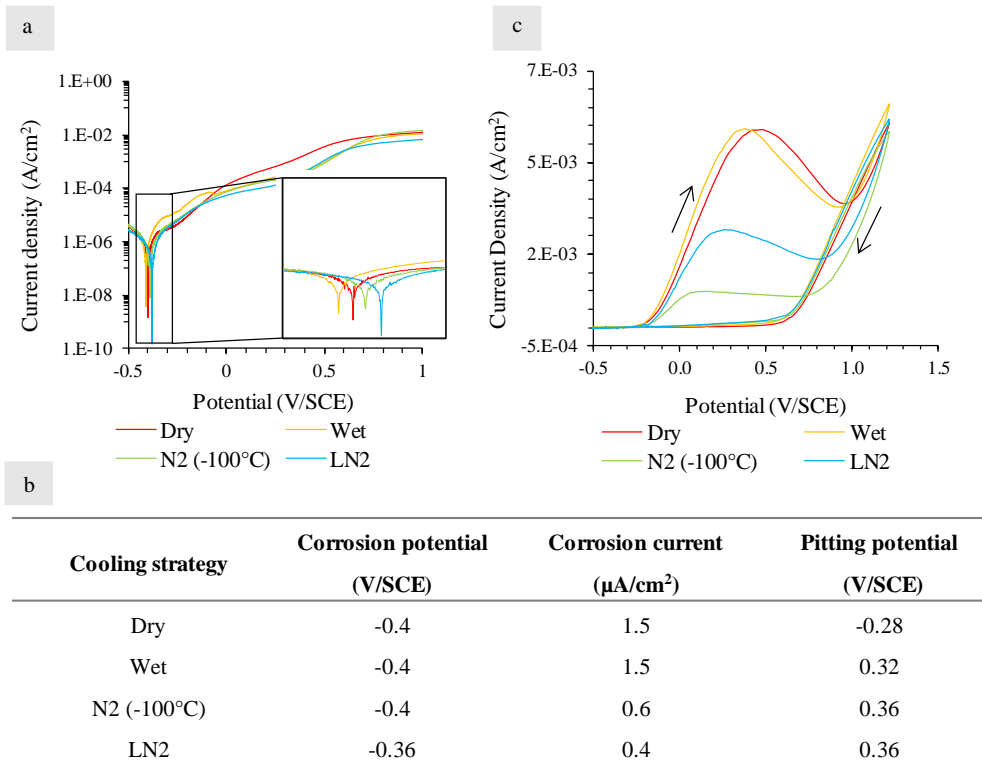


Fig. 3. a) Potentiodynamic polarization curves in IGENALN at 37°C as a function of the cooling strategy; b) corrosion potentials and corrosion current densities recorded in IGENALN at 37°C as a function of the cooling strategy; c) cyclic polarization curves in IGENALN at 37°C as a function of the cooling strategy.

#### 4. Conclusions

The paper investigated the effect of different machining cooling strategies on the corrosion resistance of the AISI 316L stainless steel used for reusable medical devices.

In particular, both LN2 cooling and a novel cooling strategy that makes use of N2 cooled at -100°C were investigated, while dry and wet cutting were used as baseline.

The following considerations may be drawn:

- the machined surfaces presented a deeper, harder and more compressed sub-surface layer when low-temperature coolants were applied;
- dry cutting favored the highest formation of defects on the machined surfaces, while the adoption of conventional cutting fluid, LN2 and N2 contributed to obtain the opposite effect;
- both the general and localized corrosion resistances were found to be sensible to the cooling condition adopted during machining: a reduction of an order of magnitude in the corrosion current together with a less susceptibility to localized corrosion were achieved when using low-temperature coolants, which may contribute to a higher durability of the reusable devices.

On this basis, it can be stated that the use of low-temperature coolants in machining can represent an effective strategy to enhance the corrosion resistance of AISI 316L reusable medical devices exposed to the aggressive environment of the sterilization stages.



## References

- [1] I. Gurappa, *Mat. Charat.* 49 (2002) 73–79.
- [2] Q. Chen, G. A. Thouas, *Sci. Eng. R Reports.* 87 (2015) 1–57.
- [3] L. Chenglong, Y. Dazhi, L. Guoqiang, Qi Min, *Materials Lett.* 59 (2005) 3813 – 3819.
- [4] Li C, X, Bell T. *Corrosion Sci.* 48 (2006) 2035-2049.
- [5] J. Buhagiar, A. Spiteri, M. Sacco, E. Sinagra, H. Dong, *Corrosion Sci.* 59 (2012) 169-178.
- [6] F. Klocke, M. Schwade, A. Klink, D. Veselovac, A. Kopp, *Procedia CIRP* 5 (2013) 88–93.
- [7] S. Yang, O.W. Dillon, D.A. Puleo, I.S. Jawahir, *J. Biomed. Mater. Res. Part B Appl. Biomater.* 101 B (2013) 139–152.
- [8] S. Yang, Z. Pu, D.A. Puleo, O.W. Dillon, I.S. Jawahir, *Adv. Sustain. Manuf.* (2011) 177–182.
- [9] R. Bertolini, S. Bruschi, A. Ghiotti, L. Pezzato, M. Dabalà, *Biotribology* 0-1 (2017).
- [10] R. Bertolini, S. Bruschi, A. Ghiotti, L. Pezzato, M. Dabalà, *Procedia CIRP*, 65 (2017) 7–12.
- [11] A. Bordin, S. Bruschi, A. Ghiotti, P.F. Bariani, *Wear.* 328–329 (2015) 89–99.
- [12] S. Sartori, M. Taccin, G. Pavese, A. Ghiotti, S. Bruschi, *Int J Adv Manuf Technol* (2018) 1255–1264.
- [13] M.E. Fitzpatrick, A.T. Fry, P. Holdway, F.A. Kandil, J. Shackleton, L. Suominen, National Physical Laboratory Teddington, Middlesex, United Kingdom, 2005.
- [14] ASTM G5:14 Making Potentiodynamic Anodic Polarization, West Conshohocken, United States. (2017).
- [15] ASTM G61-86 Standard Test Method for Conducting Cyclic Potentiodynamic Polarization Measurements for Localized Corrosion Susceptibility of Iron-, Nickel- and Cobalt-Based Alloys, West Conshohocken, United States. (2017).
- [16] ASTM F746 Pitting or Crevice Corrosion of Metallic Surgical Implant Materials West Conshohocken, United States. (2017).
- [17] J. Kenda, F. Pusavec, J. Kopac, *J. Sci. Manuf. Eng.* 133 (2018) 1–7.
- [18] J.C. Outeiro, D. Umbrello, R. M'Saoubi, *Int. J. Mach. Tools Manuf.* 46 (2006) 1786–1794.
- [19] I. Lazoglu, D. Ulutan, B.E. Alaca, S. Engin, B. Kaftanoglu, *CIRP Annals* 57 (2008) 81–84.
- [20] G. Rotella, O.W.D. Jr, D. Umbrello, L. Settineri, *Int J Adv Manuf Technol* (2014) 47–55.
- [21] A. Shokrani, V. Dhokia, S.T. Newman, *J. Manuf. Proc.* 21 (2016) 172–179.
- [22] R. Baboian, *Corrosion Tests and Standards: Application and interpretation*, second ed., West Coshohocken PA, 1995.
- [23] L.Y. Xu, Y.F. Cheng, *Corros. Sci.* 59 (2012) 103–109.
- [24] O. Takakuwa, H. Soyama, *Adv. Chem. Eng. Sci* (2015) 62–71.
- [25] A. Turnbull, K. Mingard, J.D. Lord, B. Roebuck, D.R. Tice, K.J. Mottershead, N.D. Fairweather, A.K. Bradbury, *Corros. Sci.* 53 (2011) 3398–3415.